2013 European Control Conference (ECC)
July 17-19, 2013, Zürich, Switzerland.

PID Design by Convex-Concave Optimization

M. Hast[1], K.J. Åström[1], B. Bernhardsson[1], S. Boyd[2]

***Abstract*— This paper describes how PID controllers can be designed by optimizing performance subject to robustness constraints. The optimization problem is solved using convex-concave programming. The method admits general process descriptions in terms of frequency response data and it can cope with many different constraints. Examples are presented and some pitfalls in optimization are discussed.**

I. INTRODUCTION

Controller design is a rich problem because it requires that many factors related to performance and robustness are taken into account [18]. Many features can be captured by formulating the design problem as a constrained optimization problem [1], [7], [12], [13], [15], [17].

Convex programming [3] is a powerful optimization technique, which has guaranteed convergence and efficient algorithms that have been packaged in easy-to-use tools [5], [9]. There is a modification called convex-concave optimization which admits nonconvex criteria and constraints [4], [20]. There is in general no guarantee of convergence to a global minimum but the algorithms converge to a saddle point or local minimum.

In this paper we will consider convex-concave programming for design of PID controllers. Following the ideas in [2], [15] we consider maximization of integral gain subject to robustness constraints on the sensitivities and other constraints. Both disturbance attenuation and response time are inversely proportional to integral gain. Unconstrained maximization of integral gain does not necessarily lead to good controllers because the responses may be highly oscillatory.

PID controllers have been designed using optimization earlier with similar problem formulations [1], [7], [15]. The proposed method is similar to M-constrained Integral Gain Optimization, MIGO [10], [11], but it admits more flexible constraints and the computations are simpler. Similar approaches using linear programming can be found in [12], [13], [17], and [6] for MIMO systems. The advantages of convex-concave optimization are that the software package CVX [5], [9] allows for very compact programs, and many different criteria and constraints can be accommodated. The technique can also be extended to more complicated systems.

II. PID DESIGN

Consider a closed loop system with PI or PID control. The process transfer function is $P(s)$, and controller transfer functions are

$$C_{\text{PI}}(s) = k_p + \frac{k_i}{s}, \quad C_{\text{PID}}(s) = k_p + \frac{k_i}{s} + k_d s,$$

where k_p, k_i, and k_d are the controller parameters. A block diagram of the system is shown in Fig. 1.

Measurement noise can be reduced by a second order filter with the transfer function

$$G_f(s) = \frac{1}{1 + sT_f + s^2T_f^2/2}, \tag{1}$$

where T_f is the filter time constant. A first order filter may suffice for PI control but a second order filter is required to ensure roll-off when derivative action is used; see [1].

The combinations of the controllers and the filter transfer functions are denoted by

$$C(s) = C_{\text{PI}}(s)G_f(s), \qquad C(s) = C_{\text{PID}}(s)G_f(s).$$

Using this representation ideal controllers can be designed for the augmented plant $P(s)G_f(s)$.

A good controller should give a closed-loop system with a fast response to command signals y_{sp}, load disturbances d should be well attenuated and measurement noise should not generate too large control signals. In addition the closed-loop system should be insensitive to variations in the dynamics of the process $P(s)$.

Common criteria for control performance are the integrated error and the integrated absolute error

$$\text{IE} = \int_0^\infty e(t)dt, \qquad \text{IAE} = \int_0^\infty |e(t)|\,dt,$$

where e is the control error due to a unit step load disturbance applied at the process input or the process output or a unit step change in the command signal. The quantities IE and IAE are good measures of load disturbance attenuation for controllers with integral action. For systems that are well damped, the two criteria are approximately the same. It can be shown [1] that

$$\text{IE} = \frac{1}{k_i} \tag{2}$$

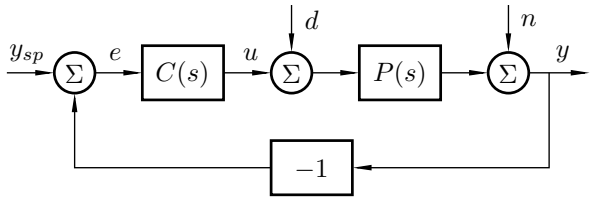

Fig. 1. Block diagram.

[1]Department of Automatic Control, Lund University, Sweden. Corresponding author: martin.hast at control.lth.se
[2]Department of Electrical Engineering, Stanford University

for a unit step disturbance and $1/(P(0)k_i)$ for a set-point step. Minimizing IE does not guarantee that the responses are satisfactory because the responses may be highly oscillatory. Combined with robustness constraints, minimization of IE may, however, give controllers with good properties [1]. That this is not always the case will be investigated in Example 4.

The sensitivity function and the complementary sensitivity functions are defined as

$$S(s) = \frac{1}{1+L(s)}, \quad T(s) = \frac{L(s)}{1+L(s)} \tag{3}$$

where $L(s) = P(s)C(s)$ is the loop transfer function. Robustness to process uncertainty can be captured by constraints on the maximum sensitivities M_s and M_t

$$M_s = \max_\omega |S(i\omega)|, \quad M_t = \max_\omega |T(i\omega)|. \tag{4}$$

Such constraints have nice geometric interpretations in the Nyquist plot of the loop transfer function. Requirements on the sensitivities mean that the Nyquist plot is outside circles; see Figure 4.15 in [1]. Process uncertainty can be represented by circles around the nominal loop transfer function. These constraints are well captured by convex-concave programming as will be shown in Sec. IV-A and IV-B.

It is important that the control actions generated by measurement noise are not too large. The fluctuations in the control signal can be computed from the transfer functions of the process and the controller and a characterization of the measurement noise, like its spectral density. Such detailed information is rarely available for PI or PID control and we will therefore use simpler measures.

The transfer function from measurement noise n to controller output for the closed loop system is

$$G_{un}(s) = C(s)S(s). \tag{5}$$

The transfer function G_{un} can be characterized by its largest value

$$M_{un} = \max_\omega |G_{un}(i\omega)|. \tag{6}$$

To ensure that measurement noise does not generate too large control actions we can introduce constraints on the transfer function G_{un}. For processes with $P(0) \neq 0$ and controllers with integral action we have $G_{un}(0) = 1$, and hence $M_{un} \geq 1$.

An approximate expression for M_{un} is the high-frequency controller gain k_d/T_f where T_f is the parameter of the noise filter (1). The parameter T_f can be determined as a compromise between noise injection and load disturbance attenuation. For a given T_f the condition is then a constraint on the derivative gain k_d which fits well into convex-concave optimization.

The constraints on noise injection can also be dealt with in this framework, design of the filter time constant can be dealt with iteratively as described in [16].

III. CONVEX-CONCAVE OPTIMIZATION

Convex-concave optimization [4], [20] is a procedure for problems where the optimization criterion and constraints are written as a difference between two convex functions,

$$\begin{array}{ll} \text{minimize} & f_0(x) - g_0(x) \\ \text{subject to} & f_i(x) - g_i(x) \leq 0 \quad i = 1, \ldots, m \end{array}$$

where f_i and g_i are convex functions. This is not a convex problem since $-g_i$ is concave. The convex functions are left unchanged and all concave functions are replaced by linearizations around the current solution point x_k, i.e., replace $f(x) - g(x)$ by

$$\hat{f}(x) = f(x) - g(x_k) - \nabla g(x_k)^T (x - x_k). \tag{7}$$

This convex approximation is an upper bound on the function being approximated. It follows that the resulting convex constraints are more conservative than the original: the feasible set will be a convex subset of the original feasible set. The new problem can be solved efficiently to produce a new feasible point x_{k+1}, and the procedure is repeated. Since the approximation is conservative, the new iterate is guaranteed to be feasible, and not to have larger objective value.

The iterative procedure converges to a saddle point or a local minimum [20]. Even though there is no guarantee of convergence to a global minimum, experience has shown the method to often be effective in producing good solutions.

IV. OPTIMIZATION

The constraints presented in the following sections will be defined frequency-wise and the considered optimization problems will have an infinite number of constraints. In order to obtain a tractable optimization problem, the problems are solved over a grid of frequency points. Since the problem is convex, a large number of constraints can efficiently be handled and a fine grid can therefore be used.

Since the convex-concave procedure is iterative there is a need for an initial controller. The initial controller needs to stabilize the system. For a stable plant it will suffice to choose the initial controller parameters to be zero but care must be taken if the process is open loop unstable; see Example 3.

The objective of the optimization is to minimize IE under robustness constraints. From (2) it can easily be seen that minimizing IE is equivalent to

$$\text{maximize } k_i. \tag{8}$$

A. Circle constraints

Consider a circle with centre c and radius r. The constraint that the Nyquist plot should lie outside the circle is equivalent to

$$r - |L - c| = r - g(\alpha) \leq 0, \tag{9}$$

where $\alpha = \begin{pmatrix} k_p & k_i & k_d \end{pmatrix}^T$. The inequality constraint (9) is a convex-concave constraint since $g(\alpha)$ is a convex function. Using (7) on (9) we obtain

$$\hat{f}(\alpha) = r - \Re\left(\frac{(L_k - c)^*}{|L_k - c|}(L - c)\right) \leq 0$$

where $\Re$ and $*$, denotes the real part and complex conjugate respectively, and L_k, is the open-loop transfer function with the controller parameters from the last iteration.

The classical robustness constraints given by the sensitivity functions imply that $L(i\omega)$ should be outside two circles with centres in $c_s = -1$ and $c_t = -M_t^2/(M_t^2 - 1)$ and radii $r_s = 1/M_s$ and $r_t = M_t/(M_t^2 - 1)$ respectively; see [1].

B. Process uncertainty

The robustness constraints can be generalized to settings with process uncertainties. Consider a process $\tilde{P}$ with uncertainties such that for each frequency point the Nyquist plot is known to lie within a circle with a frequency dependent, radius ρ, i.e.,

$$\tilde{P}(i\omega) = P(i\omega) + \Delta(i\omega), \quad |\Delta(i\omega)| \leq \rho(i\omega).$$

A constraint specifying that the Nyquist plot should lie outside a circle with centre c and radius r is then

$$r - |PC + \Delta C - c| \leq 0. \tag{10}$$

Furthermore,

$$\inf_{|\Delta|\leq\rho} \{|1 + PC + \Delta C|\} = \max(|1 + PC| - \rho|C|, 0)$$

where the equality follows from the triangle inequality and by choosing the magnitude as $|\Delta| = \min\left(\rho, \frac{|1+PC|}{|C|}\right)$ and the phase as $\arg(\Delta) = \arg(1 + PC) - \arg(C)$. Hence, (10) can be formulated as

$$r - |L - c| + \rho|C| \leq 0 \tag{11}$$

for which the concave part can be approximated in the same way as the circle constraints.

C. Curvature constraints

Minimization of IE may sometimes give Nyquist curves with very small curvature; see Example 4. A constraint on the curvature can be expressed as a convex-concave constraint. To obtain this constraint the loop transfer function is decomposed as $L(i\omega) = x(\omega) + iy(\omega)$. Furthermore, let dots denote derivatives of the corresponding variables with respect to ω. The curvature of L at a frequency point ω is then given by

$$\kappa = \frac{\dot{x}\ddot{y} - \dot{y}\ddot{x}}{(\dot{x}^2 + \dot{y}^2)^{3/2}}.$$

To avoid kinks in the Nyquist plot we introduce a constraint limiting its curvature by γ. The constraint can then be formulated as $\Im(\dot{L}^*\ddot{L}) - \gamma|\dot{L}|^3 \leq 0$, equivalent to

$$\alpha^T Q\alpha - \gamma|Z\alpha|^3 \leq 0 \tag{12}$$

where Q is an indefinite, rank one matrix. Since Q is rank one, it has only one eigenvalue different from zero, whose sign determines whether the matrix is positive semi-definite or negative semi-definite. Hence, the constraint given by (12) fits nicely into the convex-concave framework and can be written as

$$\alpha^T Q_p\alpha - \alpha^T Q_n\alpha - \gamma|Z\alpha|^3 \leq 0. \tag{13}$$

TABLE I

CONTROLLER PARAMETERS AND PERFORMANCE MEASURES FOR THE SYSTEM IN EXAMPLE 1 AND EXAMPLE 2

Optimization	k_i	IE	IAE	$y_{\max}$
Ex. 1 PI	11.54	8.67e-2	9.98e-2	17.83e-2
Ex. 1 PID	48.25	2.07e-2	3.14e-2	8.84e-2
Ex. 2 PI	7.43	13.46e-2	14.92e-2	19.45e-2
Ex. 2 PID	26.81	3.73e-2	4.63e-2	10.57e-2

where either Q_p or Q_n is zero and where the nonzero matrix is positive semi-definite. Utilizing (7), a convex approximation of (13) is given by

$$\begin{aligned} \hat{f}(\alpha) &= \alpha^T Q_p\alpha + A_k\alpha + b_k \leq 0 \\ A_k &= -\alpha_k^T Q_n - 3\gamma|Z\alpha_k|\alpha_k^T Z^H Z \\ b_k &= \alpha_k Q_n\alpha_k + 2\gamma|Z\alpha_k|^3 \end{aligned} \tag{14}$$

where H denotes the Hermitian transpose.

V. EXAMPLES

The proposed design method will be illustrated by four examples. The examples share some common features. In all examples the integral gain is maximized. The robustness constraints are $M_s = M_t = 1.4$ unless otherwise stated. A grid of 1000 logarithmically spaced frequencies between $\omega_{min} = 10^{-2}$ [rad/s] and $\omega_{max} = 10^2$ [rad/s] is used in all examples. The initial controller parameters are zero unless otherwise stated. For the examples provided, the optimization algorithm converges to a solution within seven iterations excluding the optimization problem with curvature constraints in Example 4, for which 11 iterations were needed.

Example 1. Heat conduction

An advantage of the method is that it can be applied to processes where the transfer function is only given as a frequency response or processes described by partial differential equations. We illustrate with a simple example of a process representing heat conduction where the process has the transfer function

$$P(s) = \mathrm{e}^{-\sqrt{s}}. \tag{15}$$

Maximizing integral gain with constraints on the maximum values of the sensitivity functions using the convex-concave procedure gives the following PI and PID controllers

$$C_{\text{PI}} = 2.94 + \frac{11.54}{s}, \quad C_{\text{PID}}(s) = 7.40 + \frac{48.25}{s} + 0.46s.$$

Some performance measures are given in Table I. The Nyquist plots of the loop transfer functions are shown in Fig. 2, red dashed lines for PI control and blue solid lines for PID control. The unit step load disturbance responses are shown in Fig. 3. Notice that IE is less than IAE because the responses are oscillatory. The criterion IE does not penalize oscillatory responses, on the contrary, an oscillatory response may give lower IE. The PID controller has significantly better performance than the PI controller, which is not surprising because the process (15) has lag-dominated dynamics.

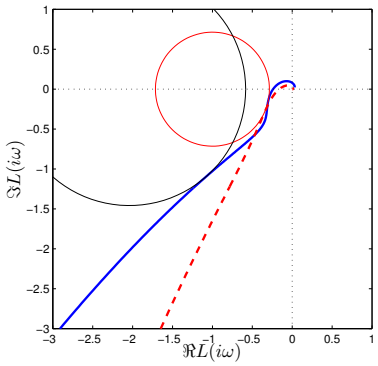

Fig. 2. Nyquist plots of the loop transfer functions for PI control (red dashed lines) and PID control (blue solid lines) of the process $P(s) = \mathrm{e}^{-\sqrt{s}}$ in Example 1. The robustness constraints $M_s = 1.4$ and $M_t = 1.4$ are shown in red and black circles.

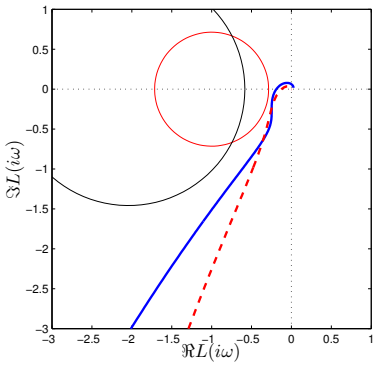

Fig. 4. Nyquist plots of the loop transfer functions for PI control (red dashed lines) and PID control (blue solid lines) of the process $P(s) = \mathrm{e}^{-\sqrt{s}}$ with 20% relative uncertainty in Example 2. The robustness constraints $M_s = 1.4$ and $M_t = 1.4$ are shown in red and black circles.

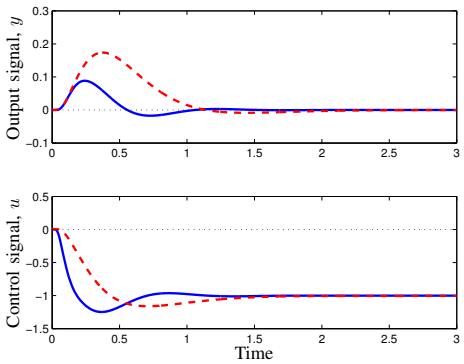

Fig. 3. Responses to a unit step load disturbances for PI (red dashed) and PID control (blue solid) of the process $P(s) = \mathrm{e}^{-\sqrt{s}}$ in Example 1.

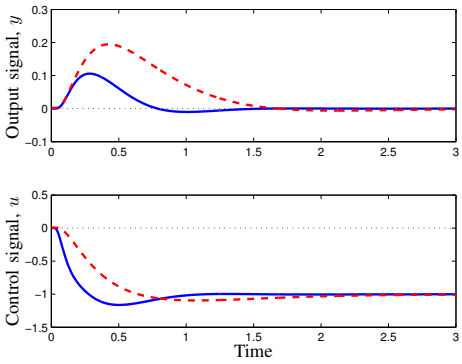

Fig. 5. Responses to a unit step load disturbances for PI (red dashed) and PID control (blue solid) of the process $P(s) = \mathrm{e}^{-\sqrt{s}}$ with 20% relative uncertainty in Example 2.

Example 2. Explicit Process Uncertainty

Process uncertainty can be accounted for explicitly as discussed in Sec. IV-B. To illustrate this we will consider the same system as in Example 1 but we will now assume that the process transfer function has a relative uncertainty of 20%. Maximizing integral gain with constraints on the maximum values of the sensitivity functions using the convex-concave procedure gives the following PI and PID controllers

$$C_{\text{PI}} = 2.37 + \frac{7.43}{s}, \quad C_{\text{PID}} = 5.74 + \frac{26.81}{s} + 0.36s.$$

Some performance measures are given in Table I. The Nyquist plots of the loop transfer functions are shown in Fig. 4, red dashed lines for PI control and blue solid lines for PID control. The unit step load disturbance responses are shown in Fig. 5.

Comparing the Nyquist plots in Fig. 2 and Fig. 4 we can see that adding uncertainties in the process model moves the Nyquist curve further away from the robustness circles in such a way that the robustness constraints are satisfied for all uncertainties in the uncertainty set. The resulting controllers obtained for the uncertain processes are less aggressive, the time responses are more sluggish and hence, the performance measures deteriorate compared with the controllers obtained in Example 1.

Example 3. Unstable Process

For unstable processes it is necessary to choose the initial controller parameters so that the loop transfer functions has the correct winding number. If the initial controller stabilizes the plant and satisfies the constraints, the winding number is preserved in the iterations if the frequency points are sufficiently dense.

To illustrate this consider PI control of an unstable process with the transfer function

$$P(s) = \frac{1}{(s-1)(1+0.1s)}.$$

The initial stabilizing controller is chosen as $C_0(s) = 6 + \frac{1}{s}$. This controller gives a loop transfer function that satisfies the encirclement condition and the constraints on the sensitivity functions as is shown in Fig. 6. The integrated error with the initial controller is $\text{IE}_0 = 1$. Maximizing integral gain with constraints on the maximum values of the sensitivity functions using the convex-concave procedure gives the PI controller

$$C_{\text{PI}}(s) = 4.67 + \frac{1.76}{s}$$

with $\text{IE} = 0.57$. Responses of the closed-loop system to a unit load disturbance at the process input are shown in Fig. 7. The responses are well damped and, hence, IE is equal to

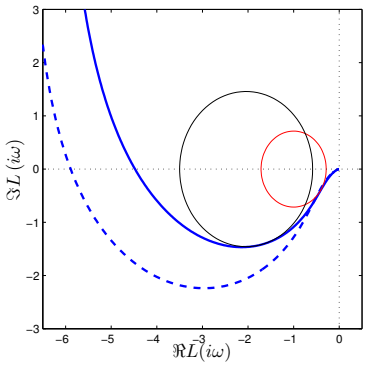

Fig. 6. Nyquist plots of the loop transfer functions for PI control of the unstable process $P(s) = \dfrac{1}{(s-1)(0.1s+1)}$ in Example 3. The robustness constraints $M_s = 1.4$ and $M_t = 1.4$ are shown in red and black circle respectively. The loop transfer function corresponding to the initial controller parameters $k_p = 6$ and $k_i = 1$ are shown in dashed curve. The loop transfer function corresponding to the optimal controller parameters $k_p = 4.67$ and $k_i = 1.76$ are shown in solid curves.

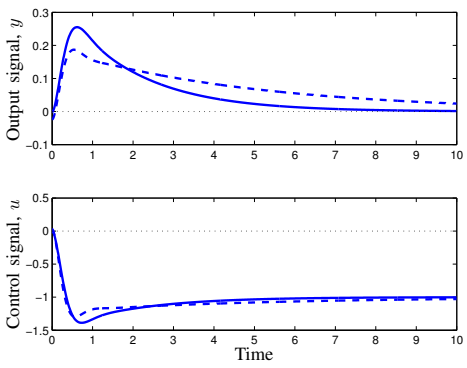

Fig. 7. Responses to a unit step load disturbances for PI control of the unstable system $P(s) = \dfrac{1}{(s-1)(1+0.1s)}$ in Example 3. The responses corresponding to the initial controller parameters $k_p = 6$ and $k_i = 1$ are shown in dashed curves. The responses corresponding to the optimal controller parameters $k_p = 4.67$ and $k_i = 1.76$ are shown in solid curve

IAE. The Nyquist plots for the loop transfer functions can be seen in Fig. 6.

Example 4. Nyquist plots with kinks

The previous examples show that minimization of IE subject to robustness constraints give controllers with good properties. However, minimizing IE does not, in general, guarantee well-behaved closed loop system; see [1]. The reason is that minimization of IE may result in closed loop systems with poorly damped oscillations. Intuitively we may expect that the tendency for oscillatory responses is counteracted by the robustness constraint. The following example shows that difficulties may indeed occur. Consider a process with the transfer function

$$P(s) = \frac{1}{(s+1)^3}. \tag{16}$$

Assuming that we only impose a constraint on the sensitivity function, maximizing integral gain using the convex-concave procedure gives the PID controller

$$C_{\text{IE}}(s) = 3.31 + \frac{6.62}{s} + 6.26s. \tag{17}$$

The poles for the closed-loop system are located in $s = -1.25 \pm 1.73i, -0.25 \pm 0.87i$ which suggests that the step responses will be poorly damped. The blue curve in Fig. 8 shows that the Nyquist plot of the loop transfer function has a kink and the corresponding time responses in Fig. 9 are highly oscillatory. This behaviour is counter-intuitive because we may expect that strong robustness constraints may induce closed loop systems with good damping. This is indeed the case for PI control but not for PID control [2], [15]. The kink will be a little smaller with tighter robustness constraints but it remains even if we require that sensitivities are less than 1.1. The problem is discussed in [1] where it is labelled the *derivative cliff*; see Figure 6.24 in [1]. The problem can be avoided in several different ways, one way is to change the criterion to IAE; see [8]. Another is to constrain the optimization so that the edges are avoided. In the MIGO design the edges are avoided by restricting the derivative gain. Other attempts to constrain the controller have also been proposed, the derivative gain has been restricted to the largest gain of a PD controller that maximizes proportional gain [1] and the constraint $T_i = 4T_d$ is proposed in [19]. When using convex-concave optimization the problem can be avoided by introducing a curvature constraint on the loop transfer function.

The Nyquist plots in Fig. 8 and the time responses in Fig. 9 also show results for two modified controllers. The green curve shows a PID controller where the derivative gain is restricted to the derivative gain of a PD controller that maximizes proportional gain with the robustness constraint. The red curve shows results where the curvature of $L(i\omega)$ is restricted to M_s.

Controller parameters and performance criteria are summarized in Table II. It is clear that the controller obtained by minimizing IE subject to robustness constraints gives oscillatory and unsatisfactory behaviour. By limiting the derivative part the oscillations are damped and IAE is reduced. The drawback with this approach is that two optimizations need to be performed. However, the performance, in terms of IAE, is better for the controller obtained by limiting the curvature of the Nyquist plot. The approach in which the curvature is limited, renders a controller whose performance is close to the controller obtained using the algorithms from [8] which minimizes IAE subject to constraints on the sensitivity functions.

VI. CONCLUSIONS

We have shown that design of PID controllers can be captured in a format that is well suited for convex-concave optimization. The criterion is to minimize IE or equivalently to maximize integral gain subject to robustness constraints. To avoid oscillatory responses we have also introduced a constraint on the curvature of the Nyquist curve of the

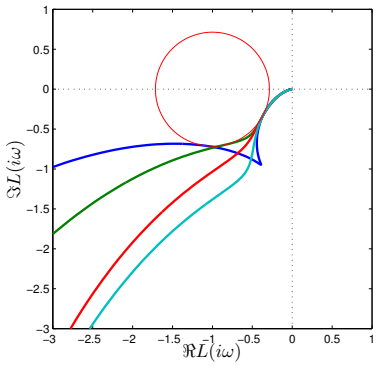

Fig. 8. Nyquist plots of the loop transfer functions for PID control of the process $P(s) = (s+1)^{-3}$ in Example 4. All curves are obtained from optimization problems where the sensitivity constraint was $M_s = 1.4$. The blue curve is obtained with no additional constraints. The green curve is obtained with the additional constraint $k_d \leq 3.82$. The red curve is obtained with the additional constraint that the curvature of the Nyquist plot is less than M_s. The cyan curve is obtained by minimizing IAE using the algorithm in [8].

loop transfer function. The optimization problems are conveniently solved using CVX, the code is very compact and additional convex-concave constraints can be included.

Since the PID controller only has three parameters the design problem can be solved by gridding. This approach [14] has the advantage that any criteria and constraints can be used. However, the complexity of gridding increases dramatically with the number of controller parameters. Convex optimization does not suffer from this difficulty and it can therefore also be applied to other controller structures such as multi-variable PID or fixed higher-order controllers.

ACKNOWLEDGMENT

This work was supported by the Swedish Research Council through the LCCC Linnaeus Center, the ELLIIT Excellence Center and the Swedish Foundation for Strategic Research through PICLU.

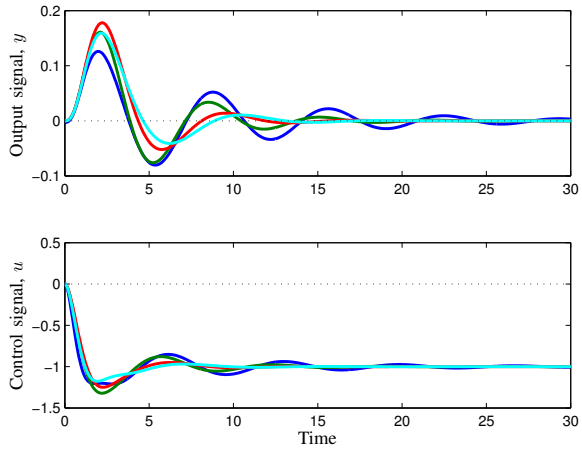

Fig. 9. Responses to unit step load disturbances for the process $P(s) = (s+1)^{-3}$ in Example 4. All curves are obtained from optimization problems where the sensitivity constraint was $M_s = 1.4$. The blue curve is obtained with no additional constraints. The green curve is obtained with the additional constraint $k_d \leq 3.82$. The red curve is obtained with the additional constraint that the curvature of the Nyquist plot is less than M_s. The cyan curve is obtained by minimizing IAE using the algorithm in [8].

TABLE II

CONTROLLER PARAMETERS AND PERFORMANCE MEASURES FOR THE SYSTEMS EXAMPLE 4.

Optimization	k_p	k_i	k_d	IE	IAE	$y_{\max}$
IE-min.	3.31	6.62	6.26	0.15	0.74	0.126
k_d-limit	3.71	4.49	3.82	0.22	0.61	0.161
κ-limit	3.61	3.20	3.34	0.31	0.57	0.178
IAE-min.	3.81	3.33	4.25	0.30	0.53	0.159

REFERENCES

[1] K.J. Åström and T. Hägglund. *Advanced PID Control*. ISA, Reasearch Triangle Park, NC, 2006.

[2] K.J. Åström, H. Panagopoulos, and T. Hägglund. Design of PI controllers based on non-convex optimization. *Automatica*, 34(5):585–601, 1998.

[3] S. Boyd and L. Vandenberghe. *Convex optimization*. Cambridge university press, 2004.

[4] Stephen Boyd. Sequential Convex Programming, 2013. *Lecture note* `http://www.stanford.edu/class/ee364b/lectures/seq_slides.pdf`.

[5] Inc. CVX Research. CVX: Matlab software for disciplined convex programming, version 2.0 beta. `http://cvxr.com/cvx`, September 2012.

[6] G. Galdos, A. Karimi, and R. Longchamp. H_∞ controller design for spectral MIMO models by convex optimization. *Journal of Process Control*, 20(10):1175–1182, 2010.

[7] O. Garpinger. Design of robust PID controllers with constrained control signal activity. Licentiate Thesis ISRN LUTFD2/TFRT--3245--SE, March 2009.

[8] O. Garpinger and T. Hägglund. A software tool for robust PID design. In *Proc. 17th IFAC World Congress, Seoul, Korea*, 2008.

[9] M. Grant and S. Boyd. Graph implementations for nonsmooth convex programs. In V. Blondel, S. Boyd, and H. Kimura, editors, *Recent Advances in Learning and Control*, Lecture Notes in Control and Information Sciences, pages 95–110. Springer-Verlag Limited, 2008. `http://stanford.edu/~boyd/graph_dcp.html`.

[10] T. Hägglund and K.J. Åström. Revisiting the Ziegler-Nichols tuning rules for PI control. *Asian Journal of Control*, 4(4):364–380, December 2002.

[11] T. Hägglund and K.J. Åström. Revisiting the Ziegler-Nichols step response method for PID control. *Journal of Process Control*, 14(6):635–650, 2004.

[12] A. Karimi and G. Galdos. Fixed-order H_∞ controller design for nonparametric models by convex optimization. *Automatica*, 46(8):1388–1394, 2010.

[13] A. Karimi, M. Kunze, and R. Longchamp. Robust controller design by linear programming with application to a double-axis positioning system. *Control Engineering Practice*, 15(2):197–208, 2007.

[14] P. Nordfeldt and T. Hägglund. Design of PID controllers for decoupled multi-variable systems. In *Proc. 16th IFAC World Congress*, Prague, Czech Republic, July 2005.

[15] H. Panagopoulos, K.J. Åstrom, and T. Hägglund. Design of PID controllers based on constrained optimisation. In *Control Theory and Applications, IEE Proceedings-*, volume 149, pages 32–40. IET, 2002.

[16] V. Romero Segovia, T Hägglund, and K.J. Åström. Noise filtering in PI and PID control. In *American Control Conference*, 2013. Submitted.

[17] M. Sadeghpour, V. de Oliveira, and A. Karimi. A toolbox for robust PID controller tuning using convex optimization. In *IFAC Conference in Advances in PID Control*, 2012.

[18] Ramon Vilanova and Antonio Visioli. *PID Control in the Third Millennium: Lessons Learned and New Approaches*. Springer Verlag, 2012.

[19] A. Wallén, K.J. Åström, and T. Hägglund. Loop-shaping design of PID controllers with constant Ti/Td ratio. *Asian Journal of Control*, 4(4):403–409, 2002.

[20] A.L. Yuille and A. Rangarajan. The concave-convex procedure. *Neural Computation*, 15(4):915–936, 2003.